http://mmg.tversu.ru ISSN 2311-1275

Mathematical Modelling and Geometry

Volume 3, No 2, p. 1 – 7 (2015)

Spectral Distributions of Localized and Delocalized States in Triple Quantum Dots with Geometry Asymmetry

I. Filikhin[a], M. Dukic, A. Karoui and B. Vlahovic

Department of Physics, North Carolina Central University, 1801 Fayetteville Street, Durham, NC 27707, USA

e-mail: [a] ifilikhin@nccu.edu

Received 1 July 2015. Published 15 July 2015.

Abstract. Electron localization and tunneling in triple quantum dot (TQD) are studied and the electron energy spectrum is deduced. Laterally distributed InAs/GaAs TQDs were modeled using single sub-band effective mass approach with effective potential simulating the strain effect. Electron localization dynamics in TQD over the whole spectrum is studied by varying the inter-dot distances. The effect of adding a third dot to a double quantum dot (DQD) is investigated as a weakly coupled system. Triangular and linear chain configurations of TQDs are considered. We show that the presence of a third dot increases the tunneling in the DQD and that the tunneling is sensitive to small violations of the TQD mirror symmetry.

Keywords: quantum dots, electron states, single-electron tunneling

PACS numbers: 73.21.-b, 73.21.La, 73.23.Hk

This work is supported by NSF (HRD-1345219).

1. Introduction

Due to their unique properties, semiconductor heterostructures, such as quantum dots (QDs) and rings are of great interest for the development of new nano-devices. The ability to grow dense and uniform QD assemblies offers new ways for making new generation of quantum devices. However, there are fundamental issues associated with the practical use of QD assemblies. Actually, imperfections in real world QD assemblies impede making efficient QD based devices, and QD assemblies perform rather poorly. For instance, QD based third generation solar cells have efficiencies much lower than theoretical predictions [1, 2, 3] and even worse than QD-less photovoltaic devices. Also, QD based optical and quantum computing devices are impractical as of yet, despite the varieties of theoretical studies and device design. Generally, the relation between tunneling and chaos is an inalienable phenomenon in the meso- and nano- world [4]. Known fabrication technologies yield dissymmetric quantum dots. This suggests a chaotic behavior within the QDs, which has a strong influence on the charge transport and other properties [5]. Primary steps for studying large QD assemblies, consisted in studying Double Quantum Dots (DQDs), triple quantum dots (TQDs), QD rings, and QD chains. Recently it has been demonstrated [6] that electron localized and delocalized states and the tunneling in double quantum dots (DQDs) are highly sensitive to the violation of the geometrical symmetry of DQD (see also [7]). In present work, we study single electron localization and tunneling in triple quantum dots (TQDs), which have been given great attention in connection to charge transport through nono-scaled systems [8, 9] and quantum computation problems [10, 11]. We consider the TQD as a system of a double QD weakly coupled to a third single quntum dot. Tunneling in the DQD is sudied in relation to the presence of the third QD. The weak coupling induced states make the tunneling sensitive to small symmetry violation.

2. Theoretical Model

Considering InAs quantum dots formed on a GaAs substrate, the heterostructure is modeled [12] utilizing a ***kp***-perturbation single sub-band approach. The problem is mathematically formulated by the Schrödinger equation:

$$\left(\hat{H}_{kp} + V_c\left(\mathbf{r}\right) + V_s\left(\mathbf{r}\right)\right)\Psi\left(\mathbf{r}\right) = E\Psi\left(\mathbf{r}\right),$$

where $\hat{H}_{kp}$ is the single band ***kp***-Hamiltonian operator $\hat{H}_{kp} = -\nabla\frac{\hbar^2}{2m^*}\nabla$, m^* is the electron effective mass, which depends on the radial position of the electron in the QD, thus can be written as $m^*\left(\mathbf{r}\right)$, and $V_c\left(\mathbf{r}\right)$ is the band gap potential. Inside the QD, the bulk conduction band offset is null, i.e., $V_c\left(\mathbf{r}\right) = 0$, while it is equal to V_c outside the QD. The band gap potential for the conduction band is chosen as V_c=0.594 eV. The electron effective masses in bulk InAs and GaAs are m_1^*=0.024m_0 and m_2^*=0.067m_0, respectively, where m_0 is the free electron mass. The effective

potential simulating the strain effect $V_s(\mathbf{r})$ has an attractive character and acts inside the volume of the QD [12]. The magnitude of the potential is adjusted so to reproduce experimental data. For example, the magnitude of V_s for the conduction band chosen in Ref. [13] is 0.21 eV.

To describe the tunneling of a single electron in a double quantum dot, we define the following parameter: the tunneling level $\sigma = \frac{N_{k,1}-N_{k,2}}{N_{k,1}+N_{k,2}}$ within the range of [-1,1]. $N_{k,\gamma}$ is the probability of electron localization in the Ω_γ region, where γ=1,2 refer to QD_1 and QD_2, respectively. Hence, it can be written as: $N_{k,\gamma} = \int_{\Omega_\gamma} |\Phi_k(x,y)|^2 dxdy$ for two dimensional quantum systems considered below, $\Phi_k(x,y)$ is the electron wave function for k=1,2,3,...; are the quantum numbers for the electron energy levels. The electron presence in $QD_1(\Omega_1)$ or in $QD_2(\Omega_2)$ has equal probability, since QD_1 and QD_2 have the same shape and size. For this state, the electron is delocalized and σ=0. The cases of $\sigma = 0$. The cases of $\sigma = 1$ and $\sigma = -1$ correspond to the localization of electron in QD_1 and QD_2, respectively.

3. Double Quantum Wells

A pair of adjacent discs acting as QDs are considered as two dimensional double quantum wells (DQWs). An example of experimental possibility for highly symmetric QDs (free of elongations) was reported in Ref. [14]. Dynamics of localized and delocalized states along electron spectrum in DQW with dependence on inter-dot distance has been studied in Ref. [7]. It was shown that tunneling between QWs

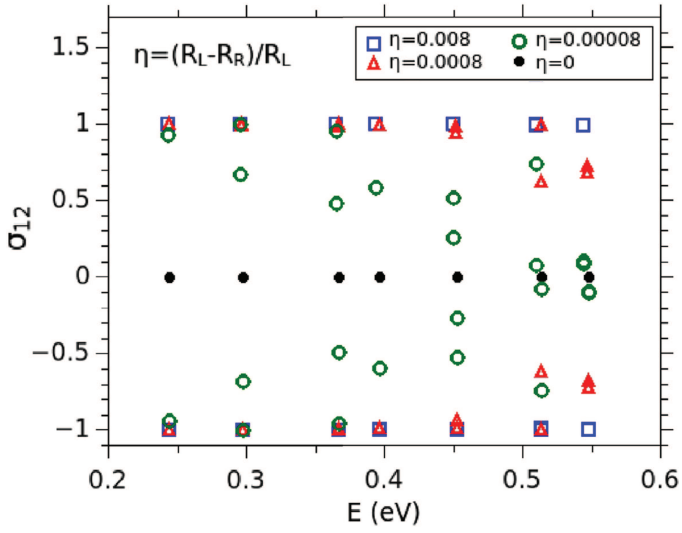

Figure 1: Localization parameter σ_{12} for DQW along the electron spectrum, as a function of the asymmetry parameter η. Violation of R-L symmetry results from the variation of the right QW radius (R_L=13 nm). The inter-dot distance is fixed to 10 nm.

occurs from high energy levels to the ground state as inter-dot distance consistently decreases. The electron spectrum appears to have three components resulting from:

localized states, delocalized states, and states with different probability for localizations in the left and the right sides of the QWs. The spectral distribution of localized (delocalized) states exhibits extreme sensitivity to small variation of QW shape, which violates Left-Right symmetry.

The sensitivity to asymmetry is illustrated in Fig. 1, where σ_{12} parameter (describes the tunneling between QD_1 and QD_2 and characterizes the localization) is shown as a function of the energy of electron confined states for different values of the asymmetry parameter $\eta = (R_L - R_R)/R_L$, where R_L and R_R are the QD radii. The initial spectral distribution for η=0 is described as completely delocalized. The small symmetry violation (e.g., η=0.8%) changes the electron probability to a completely localized distribution. It can be shown [15] that the sensitivity of the localization parameter varies as $1/(\Delta E)^2$, where ΔE is the energy difference of the same level when considered in isolated left and right QWs. This means that small variations of η have a maximal effect on electron localization when $\Delta E \simeq 0$.

4. Triple Quantum Wells

In this section we compare the spectral distribution of delocalized states in DQW and TQW. The calculations were done assuming that the QWs are identical. In the TQW, the QWs were arranged in isosceles triangular configuration (see the inset in Fig. 2b)). Both spectra in Fig. 2 confirm that the delocalization occurs

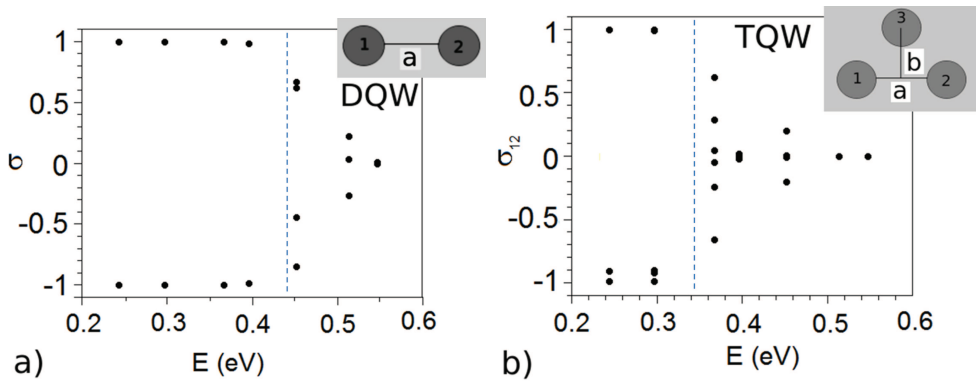

Figure 2: σ-parameter and electron spectrum of: a) DQW, inter-dot distance is a=36 nm, and b) TQW configured as isosceles triangle (see inset) with a=37 nm and b=0. The QW radius is R=13 nm.

for high energy levels. In weakly coupled isolated DQW, the number of delocalized states in the energy spectrum consecutively decreases from the threshold shown in Fig. 2a). The effect of adding a third QW to the DQW is readily seen in Fig. 2b). It can be noted that i) the number of delocalized states in the DQW essentially increases in presence of additional QW, this intensifies the tunneling, ii) the energy for transition state is lower for TQW, i.e., 0.368 eV versus 0.452 eV, and iii) the

localized-delocalized transition is sharper for TQW. The number of delocalized states is larger for $\sigma \simeq 0$.

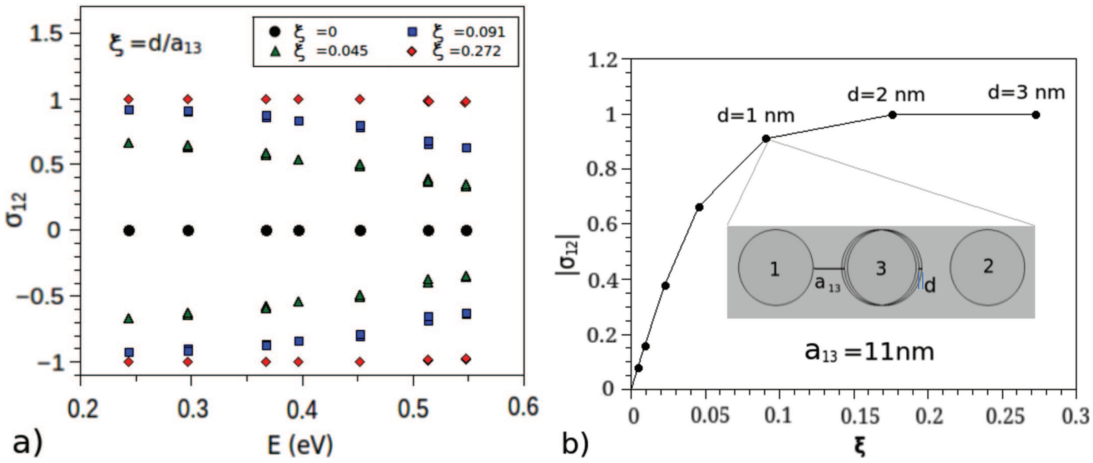

Figure 3: a) σ_{12}- parameter of localization defined for the QD_1 and QD_2 pair in the TQW along with the electron spectrum. Inter-dot distance is a=37 nm and b=0, which makes the TQW a linear chain of QWs. Results for different asymmetry $\xi = d/a_{13}$ defined by d, the shift of QD_3 relative to the QD_1 - QD_2 midpoint. The solid circles correspond to d=0. b) Magnitude of the localization parameter $|\sigma_{12}|$ for the electron ground state, as a function of ξ, the QD_3 position asymmetry within TQW. The inset shows the chain configuration TDW (a_{13}=11 nm, a_{12}=48 nm).

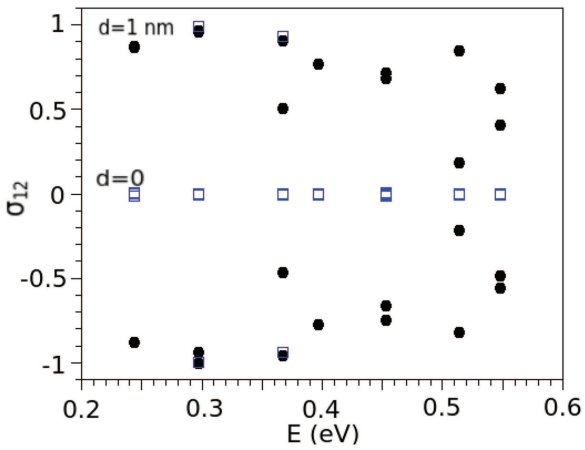

Figure 4: σ_{12}-parameter along with the electron energy spectrum for a triangular TQW. The inter-dot distance is a=37 nm and the triangle height is b=23 nm. The data is obtained for different values of the TQW asymmetry, $\xi = d/a_{13}$ defined by d the shift of QD_3 position relative to the triangle upper vertex. Open squares (solid circles) are for d=0 nm (d=1 nm, ξ=0.092).

To further compare the effect of symmetry violation both by QW shape and

position within the TQW complex, a linear distribution of identical QWs is explored. Results of calculations for σ_{12} are shown in Fig. 3a), for different values of asymmetry parameter $\xi = d/a_{13}$, being defined by d, the shift of QW_3 (relative to QW_1-QW_2 midpoint), and a_{13} (QW_1-QW_3 separation distance). The subscripts refer to considered QW. The TQD configuration is illustrated in the inset of Fig. 3b). The initial electron state is localized state for all confinement levels and σ_{12}=0. The tunneling to delocalized state is suppressed when ξ is larger than 0.1, as shown in Fig. 3. The threshold for delocalization suppression differs for different parts of the spectrum. For low-lying levels, the localized state is reached with smaller values of asymmetry ξ. Comparing Fig. 1 and 3, one can conclude that the high sensitivity of tunneling to DQW symmetry violations does not take a place with TQD configuration change (through the shift of QW_3 location). Similar result was obtained for TQW with triangular configuration, as shown in Fig. 4. The tunneling from delocalized to localized state occurs when the asymmetry is larger than 9%.

5. Conclusion

We studied the dynamics of localized-delocalized states and electron spectra in TQWs. The effects of adding a third QW to a pair on the electron localization in the system were considered. We showed that the tunneling increases in presence of an additional QW. Two types of Left-Right symmetry violation in triple QW have been proposed: by QW position deviation and/or by QW shape-size deviation. We found that the tunneling is sensitive to the position of the third QW relative to the pair. Also, we showed that the tunneling in DQW is extremely sensitive to extremely small asymmetrical variations of the QW shapes. Such sensitivity is technologically important for future quantum devices as well as next generation photovoltaic cells.

References

[1] Luque A., Marti A., and Stanley C. *Understanding intermediate-band solar cells*. Nature Photonics 2012, **6**, p. 146

[2] Beard M.C., Luther J.M. and Nozik A.J. *The promise and challenge of nanostructured solar cells*. Nature Nanotechnology, 2014, **9**, p. 951

[3] Nozik A.J., Beard M.C., Luther J.M., Law M., Ellingson R.J., and Johnson J.C. *Semiconductor Quantum Dots and Quantum Dot Arrays and Applications of Multiple Exciton Generation to Third-Generation Photovoltaic Solar Cells*. Chem. Rev. 2010, **110**, p. 6873

[4] Nakamura K. and Harayama T. *Quantum Chaos and Quantum Dots*. Oxford: Oxford University Press, 2004, 216 pp

[5] Ponomarenko L.A., Scheidin F., Katsnelson M.I., Yang R., Hill E.W., Novoselov K.S., and Geim A.K., *Chaotic Dirac Billiard in Graphene Quantum Dots*. Science 2008, **320**, pp. 356 – 358

[6] Filikhin I., Matinyan S.G., and Vlahovic B. *Electron Spectrum, Localization and Tunneling in Double Nanoscale Structures*. Mathematical Modelling and Geometry 2014, **2**, pp. 1 – 8

[7] Bleibaum O., and Belitz D. *Weak localization of electrons in an external electric field*. Phys. Rev. B 2004, **69**, 075119-10

[8] Gaudreau L., Sachrajda A.S., Studenikin S., Kam A., Delgado F., Shim Y.P., Korkusinski M., and Hawrylak P. *Coherent transport through a ring of three quantum dots*. Phys. Rev. B 2009, **80**, 075415

[9] Taranko R. and Parafiniuk P. *Electron transport through the triple quantum dot*. Physica E 2010, **43**, p. 302

[10] Hawrylak P. and Korkusinski M. *Voltage-controlled coded qubit based on electron spin*. Solid State Commun. 2005, **136**, p. 508

[11] He Z., Lu T. *Transport through a triple quantum dot system: Formation of resonance band and its application as a spin filter*. Phys. Let. A 2012, **376**, p. 2501

[12] Filikhin I., Suslov V.M. and Vlahovic B. *Modeling of InAs/GaAs quantum ring capacitance spectroscopy in the nonparabolic approximation*. Phys. Rev. B 2006, **73**, 205332-4

[13] Filikhin I., Suslov V.M., Wu M., and Vlahovic B., *InGaAs/GaAs quantum dots within an effective approach*. Physica E 2009, **41**, pp. 1358 – 1363

[14] Ha N., Liu X., Mano T., Kuroda T., Mitsuishi K., Castellano A., Sanguinetti S., Noda T., Sakuma Y. and Sakoda K. *Droplet epitaxial growth of highly symmetric quantum dots emitting at telecommunication wavelengths on InP(111)A*. Appl. Phys. Lett. 2014, **104**, 143106

[15] Filikhin I. and Vlahovic B. *Nano-Sensors: Search for new features*. ICNMN 2015 Miami, USA, March 9 – 10, 2015